SAND2021-10275C

The Optimal Control of Type-4 Wind Turbines Connected to an Electric Microgrid

Joseph Young
OptimoJoe
Houston, TX
Email: joe@optimojoe.com

Wayne Weaver
Michigan Technological University
Houghton, MI
Email: wwweaver@mtu.edu

David G. Wilson
Electrical Science and Experiments
Sandia National Laboratories
Albuquerque, NM
Email: dwilso@sandia.gov

Rush D. Robinett III
Michigan Technological University
Houghton, MI
Email: rdrobine@mtu.edu

***Abstract*—This research presents a supervisory optimal control framework called Oxtimal for the efficient control of Type 4 wind turbines with power quality and power system balancing metrics. This framework consists of a reduced order model (ROM) of wind turbines connected to an electrical microgrid, a discretization of the resulting constitutive equations using an orthogonal spline collocation method (OSCM), and an optimization engine to solve the resulting formulation. Using this framework, the approach is validated using wind profiles that result from high fidelity wind simulations.**

***Index Terms*—Microgrid, Wind, Turbine, Control, Optimization**

I. Introduction

Currently, there is a global effort to provide a more sustainable and secure green energy solution that helps reduce carbon-based emissions. In the United States (U.S.), large increases in renewable energy (RE) resources are planned to help meet these green energy strategies. The U.S. Department of Energy (DOE) Office of Energy Efficiency and Renewable Energy's (EERE) mission is to provide a clean energy economy (carbon-neutral) by 2050. Many new R&D goals and objectives have been initiated to realize these new technologies [1]. To that end, future energy system designs require greater system flexibility that addresses variability from a variety of sources which include all types of wind power systems [2].

Wind energys growth will require the need for advanced technology and controls to support grid resilience and integration of wind with other RE technologies [2]. The offshore wind resources along the U.S. coast lines are significant and will contribute to a rapidly growing global industry [2]. With the increase of RE systems, grid balancing requirements and disturbances will require new controls and operational techniques, especially when the dynamic stabilizing effect of conventional or spinning machine generation becomes reduced [2], [3]. New tools will be needed for the entire RE plant design and performance characteristics that can address increased variabilities and uncertainties. Integration of REs onto the electric power grid (EPG) will need to address new problems such as onshore load centers that are very distant from the generation source such as offshore wind farms [4]. Variable power flows due to REs increase the need for reactive power or energy storage system (ESS) capacity. Wind farm installations and operations will have an impact on power quality for the EPG that needs to be addressed.

Innovative approaches and advanced solutions for connecting large numbers of RE resources will need to maintain high power quality, minimize the number of power electronic components, and minimize ESS requirements. Microgrids as part of a network of power grids is a promising solution to assemble large numbers of REs on the EPG while maintaining dynamic stability and performance [5], [6]. This new technology is less tolerant to voltage quality disturbances [7] and with the widespread use of power electronic converters contribute to maintaining good power quality [8]. Numerous researchers [9], [8], [10], [11], [12], [13], [14], [15] explore a vast array of approaches to help solve these problems.

The following paper describes a control framework for a microgrid powered by wind turbines that uses an optimal control algorithm based on an on-line optimization engine with a receding horizon control. The meaning and reason behind each of these characteristics is given below.

This control framework uses the term *optimal control* since the control results from the solution of an optimization formulation that minimizes certain criteria. Given the formulation is not convex, the control framework does not guarantee a global minima, but given sufficient time it can guarantee a local minima. In practice, this minima is acceptable for control.

Even though this approach lacks a real-time guarantee, it may still be used as an on-line control. In an *on-line control*, the control framework repeatedly solves the control problem on a running system over a specified time horizon. This differs from an *off-line control*, which solves the control problem for a system not in operation. Although an on-line control requires a prediction of the future, as long as the inputs to the system can be predicted sufficiently well, it can provide a useful control.

In order to make the process of prediction and control more robust, this control framework employs a *receding-horizon control*, which is also known as a *model-predictive control*. In a receding-horizon control, the inputs that charac-

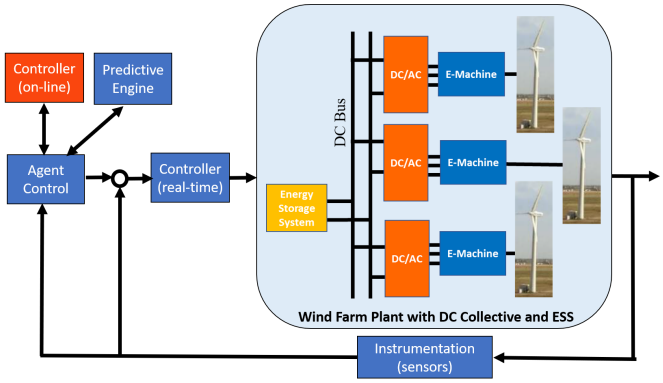

Fig. 1. Overall control architecture (wind turbine pictures courtesy of Sandia SWiFT facility [18])

terize the system are predicted over a specified time horizon and then a control over this time period is found. This time period is known as the *planning horizon*. If the actual inputs to the system differ too far from this prediction, the previously solved control is discarded and a new control is determined. This shorter time window is called the *execution horizon*.

Since an on-line control does not provide run-time guarantees, this kind of control is generally used for medium to long-term planning. For short-term control, an on-line control is typically combined with a real-time control that moderates rapidly changing dynamics.

The coordination between the different controls can be accomplished through the use of *software agents* located throughout the power system architecture. Software agents monitor the state of the system through the use of sensors, determine the appropriate course of action, and then influence the system behavior by advising the different controllers. The use of software agents for power system control continues to evolve. Recently, there has been emphasis on single agent control strategies coupled with team level strategies [16]. Wilson et al. describe one such methodology for combining these controllers [17] and a simplified diagram of how these components interconnect can be found in Figure 1. While these interactions are important, this paper focuses on the longer term plan through the use of the optimal control used by the on-line control.

The methodology presented in this paper can be compared to the techniques used by a variety of different teams. Park et al. studied the use of a model predictive control for shipboard power management systems [19]. There, the authors use an integrated perturbation analysis and sequential quadratic programming (IPA-SQP) solver from Ghaemi, Sun, and Kolmanovsky [20] to find a control that determines how power is used within the system. The framework presented here differs from Park et al. in that their work attempts to find a real time controller, but sacrifices optimality in the case where the perturbation in the initial conditions is too large. The framework under discussion finds an optimal solution, but provides no real-time guarantees and must be used on-line. Both methodologies also differ in the reduced-order model used for their respective analyses.

Abhinav et al. [21] present an optimization strategy for the frequency synchronization of multiple AC microgrids. In their approach, they formulate the control as a convex optimization problem, which is solved using the Alternative Directional Multiple of Multipliers (ADMM). The framework here differs from their approach in that their work focuses on synchronization of AC microgrids and this framework focuses on the overall operation of DC microgrids. Next, their work uses distributed optimization algorithms whereas this framework uses a parallel, nonlinear optimization solver. In addition, while both methodologies use a circuit based reduced order model, they differ in the actual model used.

The framework described in this document improves upon the reduced order model, discretization, and optimization used by Wilson et al. [22], [23], [17], Young, Cook, and Wilson [24], Weaver et al. [5], and Hassel et al. [25]. In this paper, the reduced order model of the electrical microgrid is both simplified and generalized by combining the microgrid components into an alternating sequence of series and parallel circuit components that represent the power system. Next, the discretization is improved from a finite difference method to an orthogonal spline collocation method. This allows for improved model fidelity and state control. Finally, this resulting formulation is solved using faster, more powerful algorithms from a prototype version of Optizelle [26], which implements an inexact composite-step SQP method combined with a primal-dual interior point method. This allows the model fidelity to be improved by over an order of magnitude. Nevertheless, the formulation is generic and other nonlinear optimization algorithms and software can be applied. However, their performance is not examined here.

This current approach to control was first described in a paper by Young, Wilson, and Cook [27]. This paper improves upon and differs from that work in two key respects. First, it changes the application from a shipboard power system to a small wind farm collective in an effort to demonstrate the broadly applicable nature of the reduced-order model as well as the control framework. Second, it presents and demonstrates how nonlinear bounds can be implemented and applied to the state variables within the control formulation. This last feature is somewhat unusual for an optimal control due to the difficulty in implementing such a feature in a more traditional differential equation solver such as a Runge-Kutta method.

Finally, this work is being presented in conjunction with a separate paper from Young, Wilson, Weaver, and Robinett [28] that details a similar approach to the control of a microgrid supplied by PV arrays. Though related, these two papers differ in the reduced-order models used and objective sought by the optimal control formulation.

The paper is divided into six sections. In Section II, the paper introduces the reduced order model used to represent the microgrid. In order to discretize these equations, Section III describes the orthogonal spline collocation method. Using the fully discretized dynamics, Section IV formulates the optimal control. Then, using the completed framework, Section V describes the application of the optimal control to a small wind farm collective. Finally, Section VI summarizes the paper's findings.

II. Reduced Order Model

To model an electrical microgrid, this control framework represents the microgrid as a circuit using Kirchoff's circuit laws. Similar to the work of Wilson et al. [22], [23], [17] and Young, Cook, and Wilson [24], [27], the model is comprised of a parallel DC circuit in Figure 2 connected to multiple wind turbines in Figure 3. In these diagrams, components outlined in dotted squares are optional. In addition, the wind turbine circuit is transformed into the dq0 reference frame.

In this reduced order model, power generation is represented as either a constant current source in a parallel component or as a wind turbine. As far as storage, it is represented using the variable u and is present either as a voltage source in a wind component or as a current source in a parallel DC component. In the parallel DC component, the variable P represents a direct power load that removes a specified amount of power from the system, which models the load from a given device. In a similar manner, d represents a kind of *dispatchable load*. Like P, it removes power from the system, but the controller is given the ability to softly meet a load demand, D. This means that the control may provide more or less power at any particular instance with the overall goal of providing the same amount of energy over the entire planning horizon. In addition, the current source i_{obj} represents a controllable power sink used to pull power from a wind turbine or other component to a specified bus. This is used by the objective in the optimal control. In the wind turbine component, the variable λ denotes the duty cycle in an average-mode model of the stator power converter connected to the DC bus. Next, p denotes the number of pole pairs, N the gearbox ratio, ω_s the stator or synchronous frequency, ω_r the rotor frequency, R_m the blade radius, v_m the wind velocity, and C_m the power coefficient for the turbine. Note, the stator frequency is controlled and is therefore a variable in this formulation. In terms of connectivity, the DC parallel component may accept any number of sources and sinks whereas the wind component contains a single sink.

Using these components, the state dynamics for the parallel DC components are represented as

$$\begin{aligned}\textstyle\sum[\lambda_{src}]i_{src} + [u] = \\ \textstyle\sum[\lambda_{snk}]i_{snk} + Cv' + \frac{v}{R} + \left[\frac{P}{v}\right] + \left[\frac{d}{v}\right]\end{aligned} \tag{1}$$

$$v = \text{const} \tag{2}$$

$$w' = -vu \tag{3}$$

$$w(0) = w_0 \tag{4}$$

$$0 \le w \le w_{\max} \tag{5}$$

$$0 \le d \tag{6}$$

and the wind turbine components as

$$\begin{aligned}L_s i'_{s_d} + L_m i'_{m_d} + R_s i_{s_d} \\ -\omega_s(L_s i_{s_q} + L_m i_{m_q}) + \lambda v_{snk_d} = [u_d]\end{aligned} \tag{7}$$

$$\begin{aligned}L_s i'_{s_q} + L_m i'_{m_q} + R_s i_{s_q} \\ +\omega_s(L_s i_{s_d} + L_m i_{m_d}) + \lambda v_{snk_q} = [u_q]\end{aligned} \tag{8}$$

$$\begin{aligned}L_r i'_{r_d} - L_m i'_{r_d} + R_r i_{r_d} \\ -(\omega_s - pN\omega_r)(L_r i_{r_q} - L_m i_{m_q}) = 0\end{aligned} \tag{9}$$

$$\begin{aligned}L_r i'_{r_q} - L_m i'_{r_q} + R_r i_{r_q} \\ +(\omega_s - pN\omega_r)(L_r i_{r_d} - L_m i_{m_d}) = 0\end{aligned} \tag{10}$$

$$i_{r_d} + i_{m_d} = i_{s_d} \tag{11}$$

$$i_{r_q} + i_{m_q} = i_{s_q} \tag{12}$$

$$J\omega'_r + B\omega_r + L_m pN(i_{r_d} i_{s_q} - i_{s_d} i_{r_q}) = \tau_r \tag{13}$$

$$\tau_r\omega_r = \frac{1}{2}\pi\rho R_m^2 v_m^3 C_m\left(\frac{R_m}{v_m}\omega_r\right) \tag{14}$$

$$i_{s_d}(0) = i_{s_{d_0}} \tag{15}$$

$$i_{s_q}(0) = i_{s_{q_0}} \tag{16}$$

$$i_{r_d}(0) = i_{r_{d_0}} \tag{17}$$

$$i_{r_q}(0) = i_{r_{q_0}} \tag{18}$$

$$i_{m_d}(0) = i_{m_{d_0}} \tag{19}$$

$$i_{m_q}(0) = i_{m_{q_0}} \tag{20}$$

$$\omega_r(0) = \omega_{r_0} \tag{21}$$

$$i_{s_m}^2 = \frac{2}{3}(i_{s_d}^2 + i_{s_q}^2) \tag{22}$$

$$i_{r_m}^2 = \frac{2}{3}(i_{r_d}^2 + i_{r_q}^2) \tag{23}$$

$$i_{m_m}^2 = \frac{2}{3}(i_{m_d}^2 + i_{m_q}^2) \tag{24}$$

$$i_{s_{m_{\min}}} \le i_{s_m} \le i_{s_{m_{\max}}} \tag{25}$$

$$i_{r_{m_{\min}}} \le i_{r_m} \le i_{r_{m_{\max}}} \tag{26}$$

$$i_{m_{m_{\min}}} \le i_{m_m} \le i_{m_{m_{\max}}} \tag{27}$$

$$i_{dc}v_{dc} = i_{s_d}v_d + i_{s_q}v_q \tag{28}$$

$$v_{dc}^2 = \frac{2}{3}(v_d^2 + v_q^2) \tag{29}$$

$$w' = -u_d i_{s_d} - u_q i_{s_q} \tag{30}$$

$$w(0) = w_0 \tag{31}$$

$$0 \le w \le w_{\max} \tag{32}$$

$$0 \le \lambda \le 1. \tag{33}$$

In these equations and bounds, square brackets denote elements that may be present or not present depending on the configuration of the grid. As a note for the DC parallel component, since the control framework holds v constant, the capacitor C becomes vestigial and the resulting formulation becomes a differential algebraic equation (DAE.) As a result, holding v constant does create some difficulty since the resulting system may not necessarily be feasible without enough fidelity in the available controls. Most often, this can be ensured by requiring that there exist more control than state variables after discretization modulo bounds on the control variables.

In summary, the control framework employs a reduced order model comprised of a parallel DC circuit connected to multiple wind turbine components. These components are highly configurable and allow a microgrid that contain a various assortment of generation, loads, voltages, and storage devices to be quickly assembled.

III. Discretization

In order to satisfy the dynamics described in the previous section, the control framework uses an Orthogonal Spline Collocation Method (OSCM.) Properties of this approach are described by de Boor and Swartz in [29]. In short, an OSCM represents each unknown function as a Hermite cubic spline with unknown coefficients. These coefficients become the

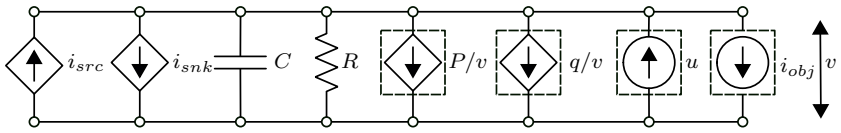

Fig. 2. Parallel DC Component

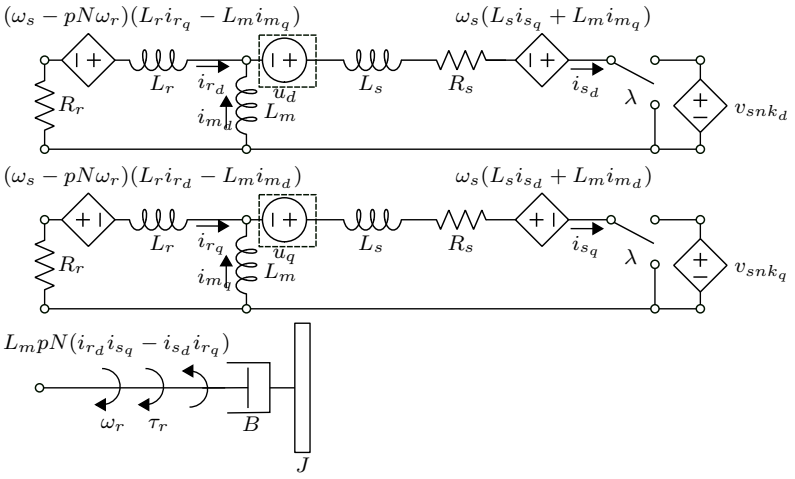

Fig. 3. Wind Turbine Component

variables in the optimization formulation. The polynomials that constitute these splines are given by

$$h_{00}(t) = (1+2t)(1-t)^2 \tag{34}$$
$$h_{10}(t) = t(1-t)^2 \tag{35}$$
$$h_{01}(t) = t^2(3-2t) \tag{36}$$
$$h_{11}(t) = t^2(t-1). \tag{37}$$

Then, the control framework attempts to satisfy the dynamics at specified points called collocation points. When the collocation points correspond to Gaussian quadrature points, the OSCM converges to the true solution of the DAE at the rate $O(h^4)$ where h denotes the largest interval in the mesh used by the Hermite cubic spline.

In order to assemble the system of equations required for optimization, the control framework employs an assembly scheme similar to the one used by older versions of Chebfun [30], [31]. It accomplishes this by creating and utilizing a combination of evaluation operators, E, and differentiation operators, D, that map the coefficients of a Hermite cubic spline to the evaluation of that spline, or its derivative, at the collocation points defined by the spline's mesh. In other words, the domain of these operators is the space of coefficients of the spline and the codomain is either the evaluation or derivative at the collocation points. For example, the differential equation

$$u' = -u \tag{38}$$

is discretized as

$$D\alpha = -E\alpha \tag{39}$$

where α represents the coefficients of the spline. Note, this example does not impose boundary conditions, but these can be enforced using a similar methodology. As a note, while Chebyshev polynomials generally provide a superior approximation and model fidelity, Hermite cubic splines possess a number of desirable properties that are utilized by this control framework.

As shown by Carlson and Fritsch [32], the control framework can bound the values of a Hermite cubic spline over the entire domain by bounding the coefficients. Succinctly, the Hermite polynomial

$$p(t) = \alpha_1 h_{00}(t) + \alpha_2 h_{10}(t) + \alpha_3 h_{01}(t) + \alpha_4 h_{11}(t) \tag{40}$$

is bounded between l and u on the interval $[0, 1]$ whenever the following inequalities are satisfied

$$3l \leq 3\alpha_1 + \alpha_2 \leq 3u \tag{41}$$
$$3l \leq 3\alpha_1 - \alpha_2 \leq 3u \tag{42}$$
$$3l \leq 3\alpha_3 + \alpha_4 \leq 3u \tag{43}$$
$$3l \leq 3\alpha_3 - \alpha_4 \leq 3u. \tag{44}$$

If an upper or lower bound is undesired, simply remove that side of the inequality. Note, this approach not only allows the control variables to be bounded, but the state as well. Further, these bounds are satisfied over the entire domain and not just at the collocation or mesh points. This ensures that certain values, such as the overall power output of a generator or the capacity of a storage device, are never exceeded.

One additional benefit of using Gaussian quadrature points as collocation points is that a spline can be quickly integrated. Specifically, given the mesh $\Omega = (t_0, \ldots, t_{\text{nele}})$, spline s, and collocation points C, then

$$\int_{t_0}^{t_{\text{nele}}} s(t)dt = \sum_{k=0}^{\text{nele}-1} (t_{k+1} - t_k)(s(C_{2k+1}) + s(C_{2k+2})). \tag{45}$$

In summary, the OSCM provides a tool that allows the discretization of the reduced order model of the microgrid.

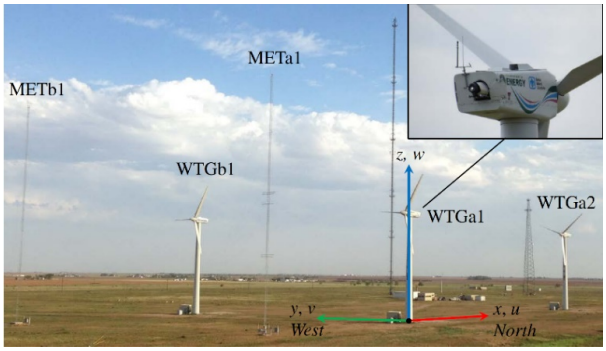

Fig. 4. Sandia Scaled Wind Farm Technology (SWiFT) facility (wind turbine pictures courtesy of Sandia SWiFT facility [18])

It is numerically stable, sparse, allows both differentiation and integration of its quantities, and can be bounded over the entire domain.

IV. Optimal Control Formulation

In order to maximize the amount of power delivered by the wind turbines, this framework focuses on maximizing the amount of power delivered to a specific DC bus. To accomplish this, the parallel DC component may specify a direct current load

$$\max \int_0^{t_{\text{end}}} i_{obj}\, dt. \tag{46}$$

In effect, this incentivizes the parallel DC component to absorb as much power as possible, which is then immediately removed through the variable i_{obj}.

Putting this all together, the optimal control formulation becomes

Maximize	Power sent to parallel DC components
Subject to	Parallel DC component dynamics
	Wind component dynamics.

To solve the above formulation, the control uses a prototype version of Optizelle [26], which implements a modified version of the composite step SQP method developed by Ridzal and Heinkenschloss [33], [34], [35]. This is combined with a primal-dual interior point method in a manner similar to NITRO described by Byrd, Hribar, and Nocedal [36]. The augmented systems that arise from this formulation are solved using a Q-less QR factorization developed by Davis [37].

V. Computational Results

In order to validate the control, a scenario based on the Sandia Scaled Wind Farm Technology (SWiFT) facility is considered [18]. A photograph of this facility can be seen in Figure 4 and a reduced order model of the facility can be seen in Figure 5. For reference, WTGa2 lies in the wake of WTGa1 by five rotor diameters (5D). The components in this reduced order model correspond to the components in Figures 2 and 3. Within these components, the following parameters are used

1) Mass moment of inertia, J - $101\,537.5 \text{kg}\,\text{m}^2$
2) Damping, B - $100\ \text{N}\,\text{m}\,\text{s}/\text{rad}$
3) Pole pairs, p - 2
4) Gearbox ratio, N - 24.12
5) Blade length plus hub radius, R_m - $13.5\ \text{m}$

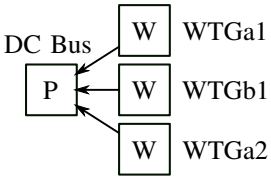

Fig. 5. Reduced order model of the SWiFT facility. P denotes a parallel DC component and W denotes a wind turbine. Base of the arrow denotes a source and the point a sink.

6) Rotor resistance, R_r - $0.007\,645\,44\ \Omega$
7) Rotor inductance, L_r - $0.007\,067\,33$ H
8) Stator resistance, R_s - $0.009\,585\,76\ \Omega$
9) Stator inductance, L_s - $0.000\,252\,35$ H
10) Initial rotor speed, ω_{r_0} - $1\ \text{rad}/\text{s}$
11) DC bus voltage, v - 460 V
12) DC bus resistance, R - $1000\ \Omega$.

For the wind profile, this scenario uses results from Nalu-Wind, which is a generalized, unstructured, massively parallel, incompressible flow solver for wind turbine and wind farm simulations. Sprague, Anathan, Vijayakumar, and Robinson [38] provide a more detailed description of their algorithm, but summarize their approach as one that includes an acoustically incompressible fluid dynamics model, two-way-coupled fluid-structure interaction (FSI), hybrid Reynolds-averaged-Navier-Stokes/LES (RANS/LES) turbulence modeling, turbine-geometry-resolved fluid meshes with mesh-motion capabilities (e.g., overset meshes), nonlinear structural dynamics models (e.g., large blade deflections), and one-way coupling to weather-scale forcing via, e.g., numerical weather prediction. Hsieh et al. [39] describe an application of Nalu-Wind to modeling turbines at the SWiFT facility.

As far as the discretization, the control framework solves for a control that lasts 600 s using a discretization with 400 elements. This gives a mesh with node boundaries every 1.5 s and results in an optimization formulation that contains 37600 constraints and 44800 variables.

In terms of the results, Figure 6 provides the wind velocity used during the scenario. In addition, the power coefficient curve can be seen in Figure 7. The actual achieved power coefficient is found in Figure 8. Notice that the optimal control effectively maximizes this value. Next, in Figure 9, the rotor frequency is seen. Notice that this value goes nearly to zero at the end of the scenario. This is due to the optimal control maximizing the amount of power delivered to the DC bus and having no information beyond the current scenario. As such, it attempts to transfer as much stored rotational energy from the turbine at the scenario's conclusion. This can be more clearly seen by examining the energy stored in the turbine in Figure 11. Generally, this can be avoided by ignoring the last few seconds of the control. Moving on to the stator, the slip frequency can be seen in Figure 12. Connecting to the DC bus, the stator duty cycle is found in Figure 13. In aggregate, the motor efficiency can be seen in Figure 14. Here, the control operates at near 98% efficiency for the leading turbines and around 96% efficiency for the turbine in the wake. Finally, the amount of power transmitted to the DC bus is found in Figure 15. Note, the voltage on the

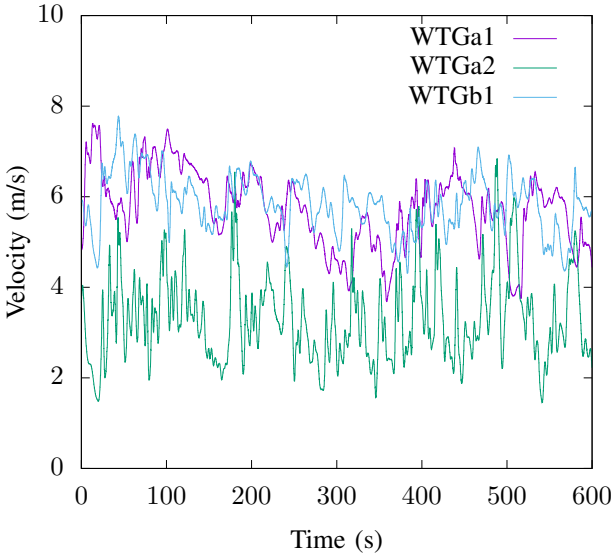

Fig. 6. Wind speed (generated from Nalu-Wind [39])

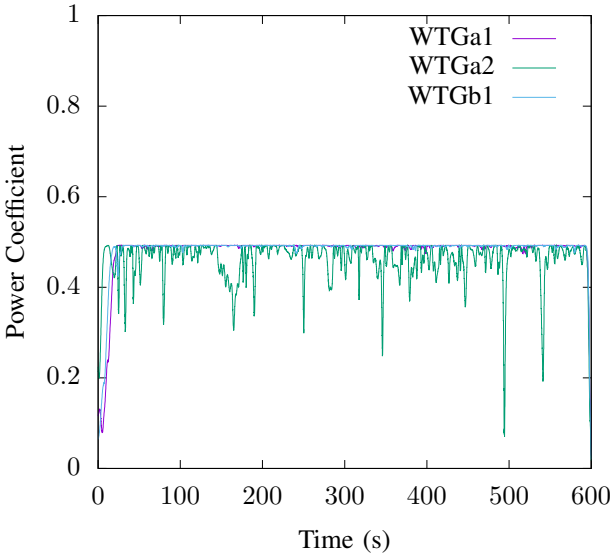

Fig. 8. Power coefficient achieved by the rotational frequency

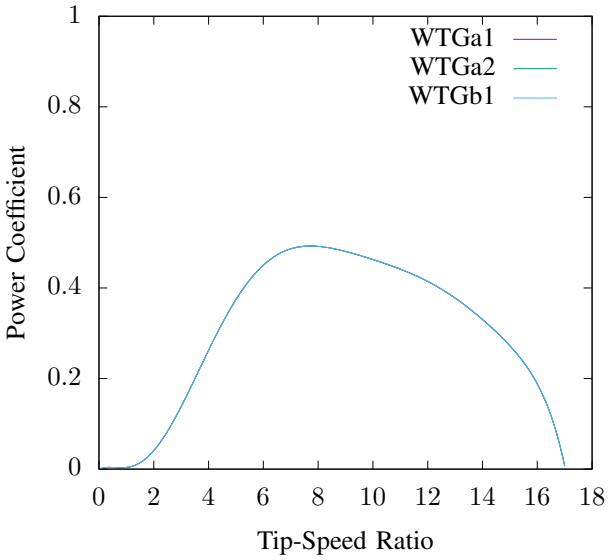

Fig. 7. Power coefficient curve

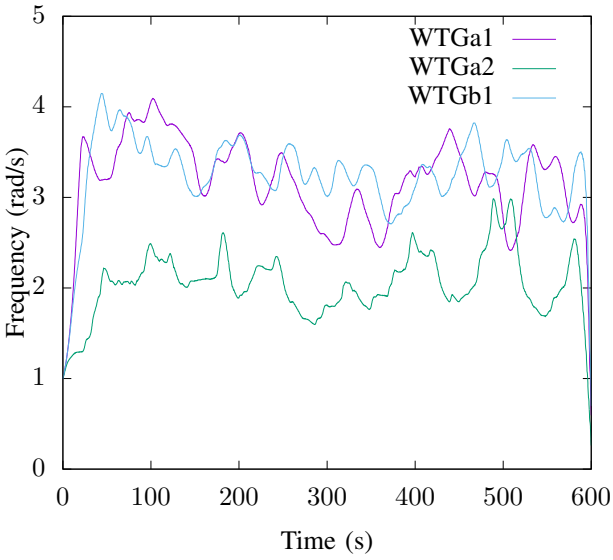

Fig. 9. Rotor frequency

DC bus is held constant and does not fluctuate throughout this scenario. In short, the control coordinates the DC bus and wind turbines effectively to maximize the amount of power delivered.

VI. Conclusions

The preceding document describes a framework for the optimal control of an electrical microgrid powered by wind turbines.

The control framework consists of a reduced-order model of an electric microgrid comprised of a collection of parallel DC circuits connected to wind turbines, a discretization based on an orthogonal spline collocation method, and an optimization engine used to solve the resulting formulation.

To validate the control framework, it is applied to a small scale wind farm driven by a high fidelity wind simulation. The resulting control demonstrates that power to the DC grid can be maximized and the wind turbines effectively coordinated where the voltage on the DC bus is held constant.

In the future, this work can be extended to work on alternative scenarios of interest as well as incorporate AC modules as part of an AC collective.

Acknowledgment

Sandia National Laboratories is a multimission laboratory managed and operated by National Technology and Engineering Solutions of Sandia, LLC., a wholly owned subsidiary of Honeywell International, Inc., for the U.S. Department of Energy's National Nuclear Security Administration under contract DE-NA0003525. The views expressed in the article do not necessarily represent the views of the U.S. Department of Energy or the United States Government. Special thanks to Dr. Jian Fu at DOE Wind Energy Technology Office for her support for this project. The

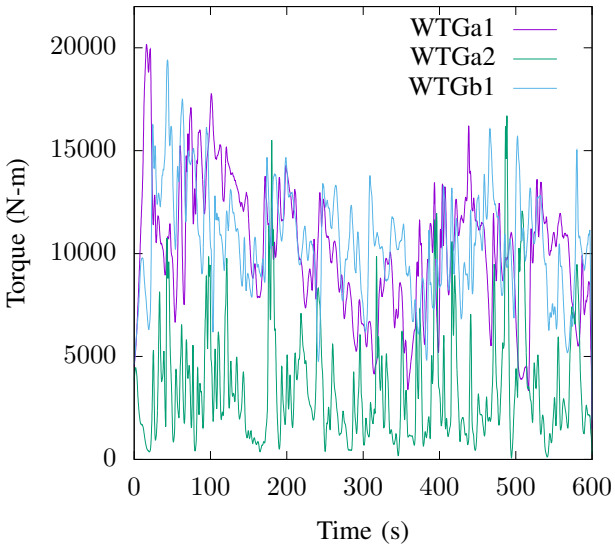

Fig. 10. Rotor torque

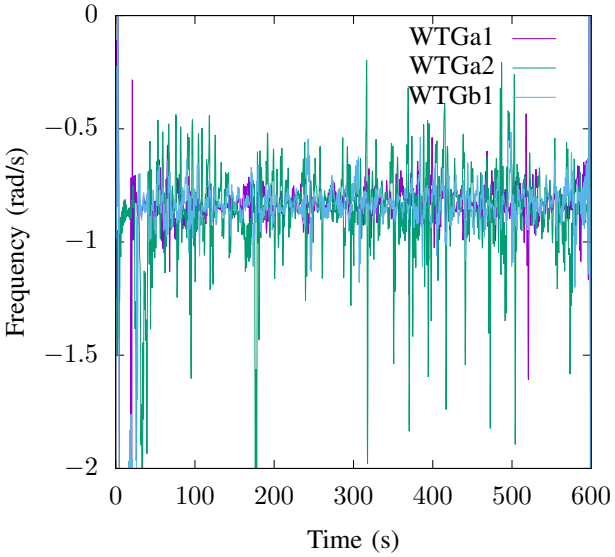

Fig. 12. Slip frequency

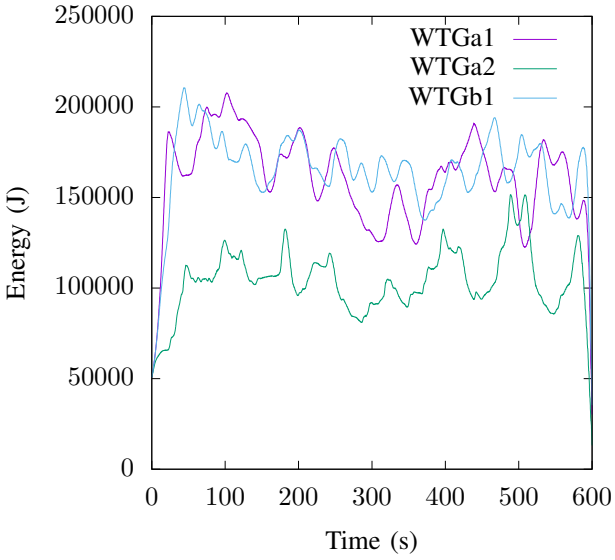

Fig. 11. Energy stored within the turbine

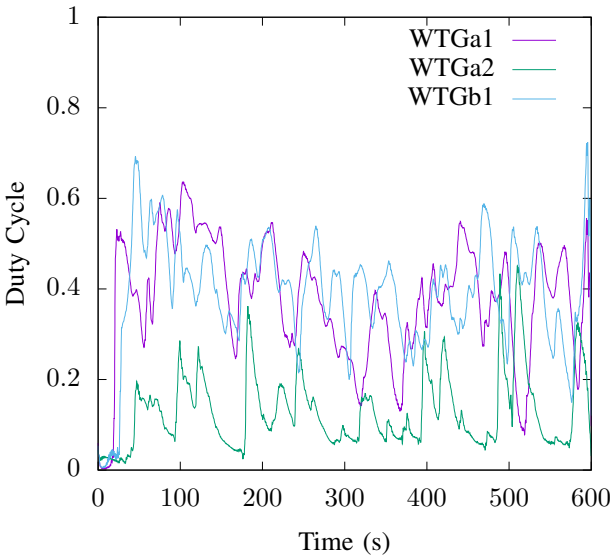

Fig. 13. Stator duty cycle

authors would also like to thank, Drs. Alan Hsieh and David Maniaci, Sandia Wind Energy Technologies department for developing the Nalu wind flow fields for the SWiFT facility and providing the corresponding wind profile inputs. This paper approved as SAND2021-XXXXC.

REFERENCES

[1] "About the office of energy efficiency and renewable energy," https://www.energy.gov/eere/about-office-energy-efficiency-and-renewable-energy, accessed: 2021-08-20.

[2] Wind Energy Technologies Office, "Multi-year program plan fiscal years 20212025," United States Department of Energy, Tech. Rep., 2020.

[3] W. Weaver, D. G. Wilson, R. D. Robinett, and J. Young, "Dc bus collection of type-4 wind turbine farms with phasing control to minimize energy storage," in *20th Wind Integration Workshop*, 2021, To appear.

[4] A. Jain, J. N. Sakamuri, and N. A. Cutululis, "Grid-forming control strategies for black start by offshore wind power plants," *Wind Energy Science*, vol. 5, no. 4, pp. 1297–1313, 2020.

[5] W. W. Weaver, R. D. Robinett, G. G. Parker, and D. G. Wilson, "Distributed control and energy storage requirements of networked dc microgrids," *Control Engineering Practice*, vol. 44, pp. 10–19, 2015.

[6] ——, "Energy storage requirements of dc microgrids with high penetration renewables under droop control," *International Journal of Electrical Power & Energy Systems*, vol. 68, pp. 203–209, 2015.

[7] V. Akhmatov, "Experience with voltage control from large offshore windfarms: the danish case," *Wind Energy*, vol. 12, no. 7, pp. 692–711, 2009.

[8] F. Blaabjerg and Z. Chen, "Power electronics for modern wind turbines," *Synthesis Lectures on Power Electronics*, vol. 1, no. 1, pp. 1–68, 2006.

[9] A. Fernández-Guillamón, K. Das, N. A. Cutululis, and A. Molina-García, "Offshore wind power integration into future power systems: Overview and trends," *Journal of Marine Science and Engineering*, vol. 7, no. 11, 2019.

[10] J. P. Daniel, S. Liu, E. Ibanez, K. Pennock, G. Reed, and S. Hanes, "National offshore wind energy grid interconnection study," ABB, Inc., Tech. Rep. DOE Award No. EE-0005365, 2014.

[11] M. Fischer, S. Engelken, N. Mihov, and A. Mendonca, "Operational experiences with inertial response provided by type 4 wind turbines," *IET Renewable Power Generation*, vol. 10, no. 1, pp. 17–24, 2016.

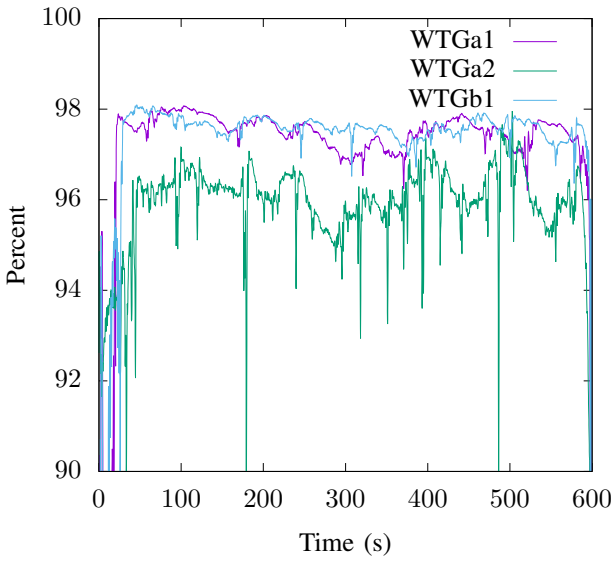

Fig. 14. Motor efficiency

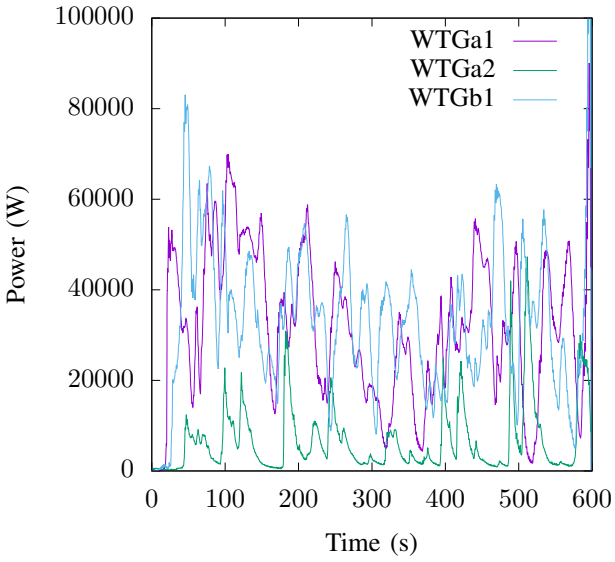

Fig. 15. Power transmitted to DC bus

[12] D. Nayanasiri and Y. Li, "Formulation of a wind farm control strategy considering lifetime of dc-link capacitor bank of type iv wind turbines," *IET Renewable Power Generation*, vol. 15, no. 12, pp. 2766–2777, 2021.

[13] L. H. Kocewiak, "Harmonics in large offshore wind farms," Ph.D. dissertation, Aalborg Universitet, 2012.

[14] A. Roscoe, P. Brogan, D. Elliott, T. Knueppel, I. Gutierrez, J.-C. P. Campion, and R. D. Silva, "Practical experience of operating a grid forming wind park and its response to system events," in *19th Wind Integration Workshop*, 2020.

[15] S. Shah and V. Gevorgian, "Control, operation, and stability characteristics of grid-forming type iii wind turbines," NREL, Tech. Rep. NREL/CP-5D00-78158, 2020.

[16] M. H. Moradi, S. Razini, and S. Mahdi Hosseinian, "State of art of multiagent systems in power engineering: A review," *Renewable and Sustainable Energy Reviews*, vol. 58, pp. 814–824, 2016.

[17] D. G. Wilson, W. Weaver, R. D. Robinett, J. Young, S. F. Glover, M. A. Cook, S. Markle, and T. J. McCoy, "Nonlinear Power Flow

[18] "Swift facility & testing," https://energy.sandia.gov/programs/renewable-energy/wind-power/wind_plant_opt/, accessed: 2021-08-20.

Control Design Methodology for Navy Electric Ship Microgrid Energy Storage Requirements," in *14th International Naval Engineering Conference & Exhibition*, 2018, pp. 1–15.

[19] H. Park, J. Sun, S. Pekarek, P. Stone, D. Opila, R. Meyer, I. Kolmanovsky, and R. DeCarlo, "Real-time model predictive control for shipboard power management using the IPA-SQP approach," *IEEE Transactions on Control Systems Technology*, vol. 23, no. 6, pp. 2129–2143, Nov 2015.

[20] R. Ghaemi, J. Sun, and I. V. Kolmanovsky, "An integrated perturbation analysis and sequential quadratic programming approach for model predictive control," *Automatica*, vol. 45, no. 10, pp. 2412 – 2418, 2009.

[21] S. Abhinav, I. D. Schizas, F. Ferrese, and A. Davoudi, "Optimization-based ac microgrid synchronization," *IEEE Transactions on Industrial Informatics*, vol. 13, no. 5, pp. 2339–2349, 2017.

[22] D. G. Wilson, J. C. Neely, M. A. Cook, S. F. Glover, J. Young, and R. D. Robinett, "Hamiltonian control design for dc microgrids with stochastic sources and loads with applications," in *2014 International Symposium on Power Electronics, Electrical Drives, Automation and Motion*, June 2014, pp. 1264–1271.

[23] D. G. Wilson, R. D. Robinett, W. W. Weaver, R. H. Byrne, and J. Young, "Nonlinear power flow control design of high penetration renewable sources for ac inverter based microgrids," in *2016 International Symposium on Power Electronics, Electrical Drives, Automation and Motion (SPEEDAM)*, June 2016, pp. 701–708.

[24] J. Young, M. A. Cook, and D. G. Wilson, "A predictive engine for on-line optimal microgrid control," in *2017 IEEE Electric Ship Technologies Symposium (ESTS)*, 2017, pp. 564–571.

[25] T. Hassell, W. W. Weaver, R. D. Robinett, D. G. Wilson, and G. G. Parker, "Modeling of inverter based ac microgrids for control development," in *2015 IEEE Conference on Control Applications (CCA)*, 2015, pp. 1347–1353.

[26] J. Young, "Optizelle – an open source software library designed to solve general purpose nonlinear optimization problems," www.optimojoe.com, 2013–2021.

[27] J. Young, D. G. Wilson, and M. A. Cook, "The optimal control of an electric warship driven by an operational vignette," in *2021 IEEE Electric Ship Technologies Symposium (ESTS)*, 2021, To appear.

[28] J. Young, D. G. Wilson, W. Weaver, and R. D. Robinett, "Supervisory optimal control for photovoltaics connected to an electric power grid," in *11th Solar and Storage Integration Workshop*, 2021, To appear.

[29] C. de Boor and B. Swartz, "Collocation at gaussian points," *SIAM Journal on Numerical Analysis*, vol. 10, no. 4, pp. 582–606, 1973.

[30] T. A. Driscoll, N. Hale, and L. N. Trefethen, *Chebfun Guide*. Pafnuty Publications, 2014.

[31] L. N. Trefethen, *Spectral Methods in MatLab*. USA: Society for Industrial and Applied Mathematics, 2000.

[32] R. E. Carlson and F. N. Fritsch, "Monotone piecewise bicubic interpolation," *SIAM Journal on Numerical Analysis*, vol. 22, no. 2, pp. 386–400, 1985.

[33] D. Ridzal, "Trust-region SQP methods with inexact linear system solves for large-scale optimization," Ph.D. dissertation, Rice University, 2006.

[34] D. Ridzal, M. Aguiló, and M. Heinkenschloss, "Numerical study of matrix-free trust-region SQP method for equality constrained optimization," Sandia National Laboratories, Tech. Rep. SAND2011-9346, 2011.

[35] M. Heinkenschloss and D. Ridzal, "A matrix-free trust-region sqp method for equality constrained optimization," *SIAM Journal on Optimization*, vol. 24, no. 3, pp. 1507–1541, 2014.

[36] R. H. Byrd, M. E. Hribar, and J. Nocedal, "An interior point algorithm for large-scale nonlinear programming," *SIAM Journal on Optimization*, vol. 9, no. 4, pp. 877–900, 1999.

[37] T. A. Davis, "Algorithm 915, suitesparseqr: Multifrontal multithreaded rank-revealing sparse QR factorization," *ACM Trans. Math. Softw.*, vol. 38, no. 1, Dec. 2011.

[38] M. A. Sprague, S. Ananthan, G. Vijayakumar, and M. Robinson, "ExaWind: A multifidelity modeling and simulation environment for wind energy," *Journal of Physics: Conference Series*, vol. 1452, p. 012071, jan 2020.

[39] A. Hsieh, D. C. Maniaci, T. G. Herges, G. Geraci, D. T. Seidl, M. S. Eldred, M. L. Blaylock, and B. C. Houchens, *Multilevel Uncertainty Quantification Using CFD and OpenFAST Simulations of the SWiFT Facility*. American Institute of Aeronautics and Astronautics, Inc, 2020.